

Fig. 2. Evolution of the ground plane of the printed quasi-Yagi Antenna, (a) Conventional printed quasi-Yagi antenna, (b) quasi-Yagi antenna with reduced ground plane, (c) quasi-Yagi antenna with modified reduced ground plane.

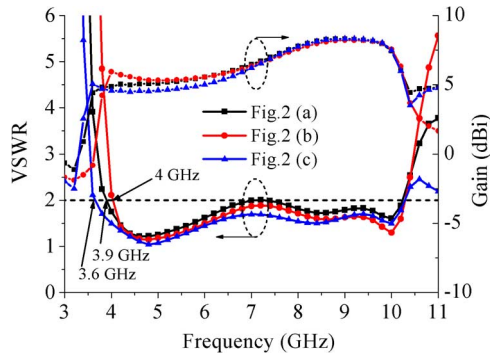


Fig. 3. Simulated VSWR and antenna gains of the three antennas shown in Fig. 2.

of the driver dipole. Compared with conventional planar quasi-Yagi antennas, the lateral size of the proposed antenna is reduced by modifying the ground plane. It is achieved by symmetrically adding two extended stubs to a flat ground plane. The microstrip line to slotline transition between the MS line and the CPS line is used to match the input impedance of the antenna to a $50\text{-}\Omega$ feeding line. In order to get a good impedance matching, a stepped microstrip feeding line is adopted. The width of the microstrip feeding line is fixed at 1.5 mm to achieve $50\text{-}\Omega$ characteristic impedance.

Fig. 2 demonstrates the evolution of the quasi-Yagi antenna ground plane. A conventional printed quasi-Yagi antenna as shown in Fig. 2(a) is used as a reference antenna. The parameters of the conventional quasi-Yagi antenna are optimized. The simulated reflection coefficient and realized gain of the conventional printed quasi-Yagi antenna is shown in Fig. 3. As shown in Fig. 3, the bandwidth defined by $\text{VSWR} < 2$ is from 3.9 to 10.25 GHz.

For conventional printed quasi-Yagi antennas, the reflector needs a larger lateral length than the length of the driver dipole for good unidirectional radiations. In order to reduce the size of the conventional printed quasi-Yagi antenna, a quasi-Yagi antenna with reduced ground plane as shown in Fig. 2(b) is employed. The width of the ground plane equals to the length of the driver dipole. It is observed from Fig. 3 that the lowest operating frequency of the antenna in Fig. 2(b) shifts toward the higher frequency, while its gain increases slightly. The reduced electrical size of the ground plane gives rise to a narrow bandwidth.

In order to increase the electrical size of the ground plane but keep the size of the antenna shown in Fig. 2(b), two stubs are symmetrically extended from its ground plane. The printed quasi-Yagi antenna with a modified ground plane is shown in Fig. 2(c). The simulated reflection coefficient and realized gain characteristics are also plotted in Fig. 3. As can be seen from Fig. 3, the lower-end $\text{VSWR} < 2$ limitation of

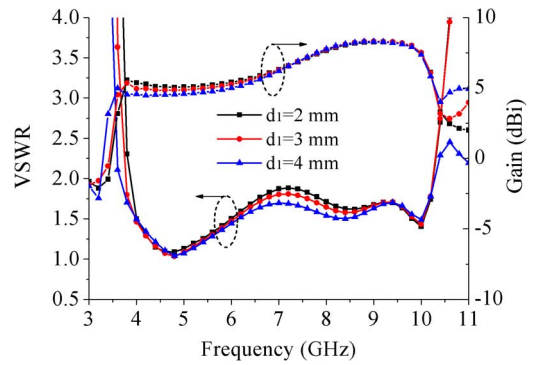


Fig. 4. Effect of the length (d_1) of stubs on the input reflection coefficients and realized gains.

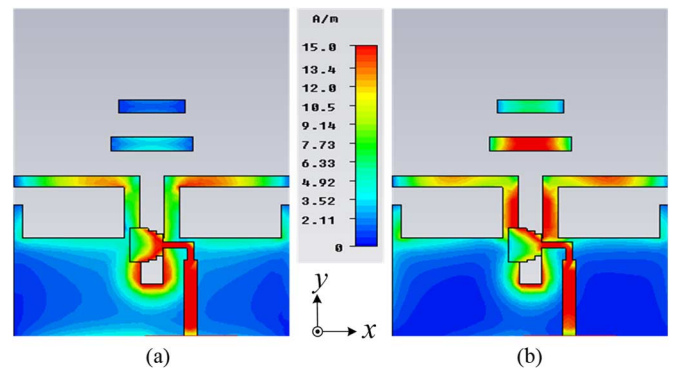


Fig. 5. Simulated surface currents distribution density of the proposed antenna at (a) 4.5 GHz and (b) 8 GHz.

the original antenna shown in Fig. 2(a) is 3.9 GHz, while the antenna with modified ground plane extends it to 3.6 GHz. This means that the bandwidth is enlarged by the modified ground plane. Obviously, the lateral length of the antenna is reduced about 16.7% compared with the conventional printed quasi-Yagi antenna shown in Fig. 2(a). This technique increases the bandwidth and miniaturizes the size of the antenna simultaneously. The price of modified ground plane is that it slightly decreases the gain at the low frequency band. The simulated antenna gain is 4.5–8.3 dBi in the band of 3.6–10.3 GHz.

Fig. 4 shows the effect of different lengths of the stubs on the reflection coefficients and the realized gains. It is observed that the impedance matching is improved as the stub length increases. However, the gain in the low frequency band decreases slightly. Thus d_1 should be optimized in order to compromise on good impedance matching and high gain.

In Yagi-Uda antenna design, metallic strip is always used as a director. In this communication, two metallic strips are used to improve directivity and impedance matching in the high frequency band. The simulated surface current distributions of the proposed antenna at 4.5 GHz and 8 GHz are shown in Fig. 5. As shown in Fig. 5(a), the surface currents on the directors are weak at 4.5 GHz. Comparing Fig. 5(b) with Fig. 5(a), the surface currents on the metallic strips are enhanced, which means that the effects of the parasitic strips as directors are improved in the high frequency band. Thus the proposed antenna works as a quasi-Yagi antenna.

In order to further illustrate the effect of the directors, their effects on the reflection coefficient and F/B ratio are plotted in Fig. 6. It is observed that the directors have great effects on impedance matching and directivity in the higher operating frequency band. The impedance

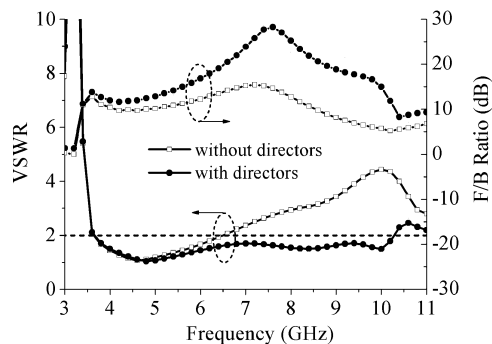


Fig. 6. Effect of the directors on the input reflection coefficient and F/B ratios.



Fig. 7. Photographs of the fabricated antenna.

matching and the directivity are significantly improved when the directors are added. Both wideband performance and good directivity are achieved.

Achieving a wide impedance matching is the main objective in the optimization procedure. The parameter optimization is mainly obtained by means of parametric analysis. The final optimized dimensions are specified as follows: $L_1 = 9$ mm, $L_2 = 7$ mm, $W_{s1} = 2.6$ mm, $W_{s2} = 2.8$ mm, $W_1 = 1.6$ mm, $W_2 = 1$ mm, $W_3 = 1.4$ mm, $W_4 = 1.6$ mm, $W_5 = 1.6$ mm, $d_1 = 3$ mm, $d_2 = 2$ mm, $d_3 = 3$ mm, $d_4 = 3$ mm, $d_s = 5.7$ mm, $d_t = 1$ mm, $S_0 = 0.7$ mm.

III. EXPERIMENTAL RESULTS

The designed antenna was fabricated with the optimized parameters. The overall dimensions of the substrate are 30 mm \times 34 mm. Fig. 7 shows the photographs of the fabricated antenna. A 50- Ω SMA connector is used to feed the antenna for measurement. The antenna performance is obtained by using an Agilent E8363B performance network analyzer (PNA) and SATIMO antenna measurement system.

Fig. 8 depicts the measured and simulated reflection coefficients of the proposed quasi-Yagi antenna. As shown in the figure, the measured and simulated results match well. The simulated impedance bandwidth defined by $VSWR < 2$ is from 3.6 to 10.3 GHz and the measured impedance bandwidth defined by $VSWR < 2$ is from 3.6 to 11.6 GHz with a ratio of about 3.22: 1. The operating bandwidth is wider than that of the antennas in [6], [7] and [11]. Clearly, this antenna can be operated in the majority of the UWB frequency band. The difference between the simulated and the measured results is due to the effect of the SMA connector and fabrication imperfections.

The realized gain variation with frequency of the antenna is shown in Fig. 9. The agreement between the measured and simulated results is good. Within the operating frequency ranging from 3.6 to 10.3 GHz, the simulated gain varies between 4.5 and 8.3 dBi, while the measured

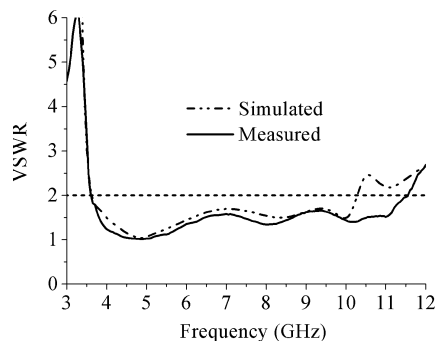


Fig. 8. Simulated and measured reflection coefficients of the proposed quasi-Yagi antenna.

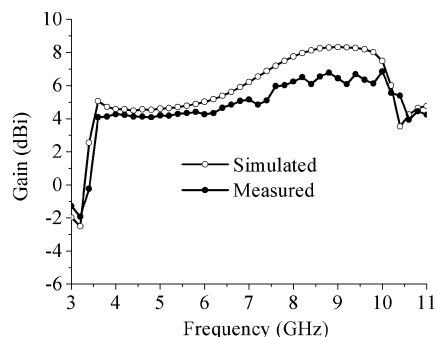


Fig. 9. Simulated and measured antenna gain of the proposed antenna.

antenna gain varies between 4.1 and 6.8 dBi. In other words, a moderate measured gain, which is better than 4 dBi, is achieved.

In order to demonstrate the radiation characteristics of the quasi-Yagi antenna, its radiation patterns are measured. The simulated and measured radiation patterns in E -plane (xoy -plane) and H -plane (yo z -plane) at 4, 6, 8, and 10 GHz are depicted in Fig. 10. It is observed from the plots that the experimental measurements have good agreement with the numerical simulations. More importantly, the main lobe of the radiation pattern is fixed to the endfire direction (y -axis direction) in the effective bandwidth. Stable radiation patterns are also obtained. Fig. 11 plots the cross-polarizations in both E -plane (xoy -plane) and H -plane (yo z -plane) at 4, 6, 8, and 10 GHz, respectively. Within the operating frequency range, the maximum cross-polarization level is -14.9 dB and -12.1 dB in the E -plane and H -plane. Moreover, the cross-polarization level in the main radiation direction is less than -15.2 dB and -15.0 dB in the E -plane and H -plane, respectively. Low cross-polarizations in both E and H -plane are achieved.

Another critical parameter for a unidirectional antenna is the F/B ratio, which represents the unidirectional radiation capability. Fig. 12 shows the simulated and measured results of the F/B ratio for the proposed quasi-Yagi antenna. As shown in the figure, the experimental measurements have good agreement with the numerical simulations. The measured F/B ratio is better than 10 dB within the band from 3.6 to 10.3 GHz. Good unidirectional characteristics are experimentally confirmed.

The linear phase response of the antenna is very important for UWB systems because a non-linear phase response will result in waveform distortion in time domain. In this study, two identical antennas were placed face to face over a distance of 300 mm [17], which maintains the far-field region condition. One antenna is used to transmit a signal and the other one is used to receive the signal. Group time delay was

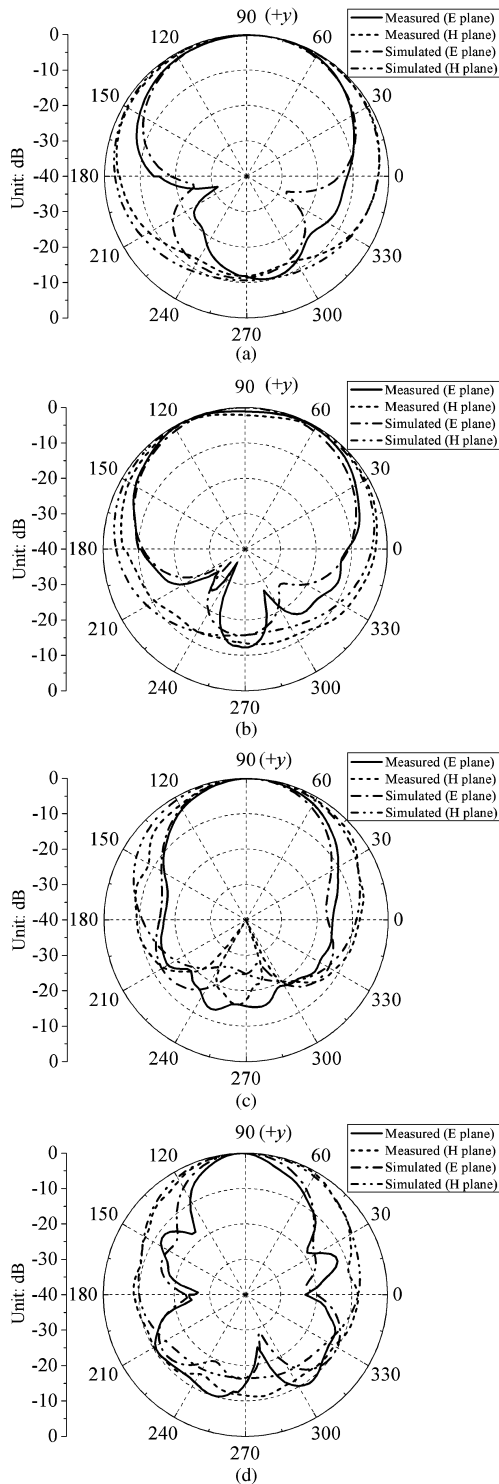


Fig. 10. Measured and simulated radiation patterns of the proposed antenna in both E-plane (xoy -plane) and H-plane (yoz -plane) at the different frequencies (a) 4 GHz, (b) 6 GHz, (c) 8 GHz, and (d) 10 GHz.

obtained by measuring the transmission coefficient via a vector network analyzer. Absorbing material is placed close to both antennas in order to avoid multiple reflections. Fig. 13 shows the simulated and measured group time delays. As shown in Fig. 13, the measured results show that the group delay of the proposed design is around 1.6 ns in the entire working band with variation less than ± 0.5 ns. Relatively flat response is achieved within the working frequency band. In other words, a good linear phase response is achieved.

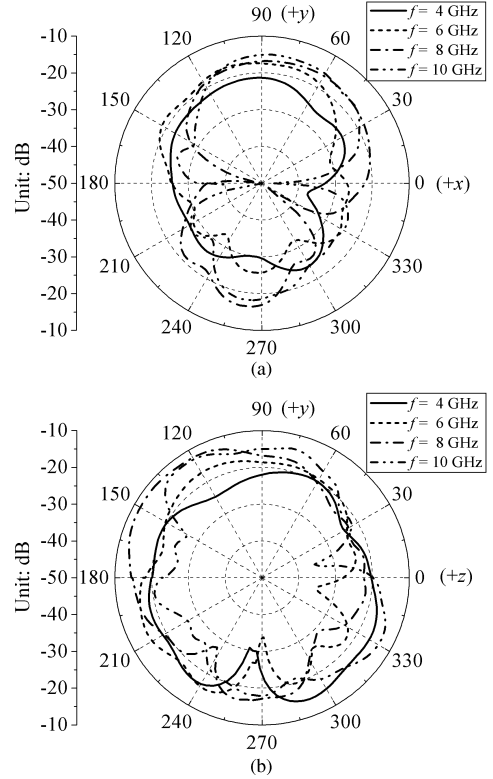


Fig. 11. Measured cross-polarization of the antenna at different frequencies (a) E-plane (xoy -plane), (b) H-plane (yoz -plane).

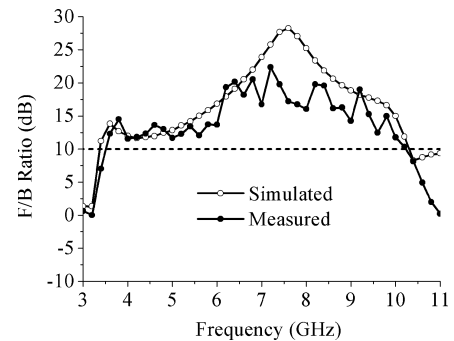


Fig. 12. Simulated and measured F/B ratios of the proposed antenna.

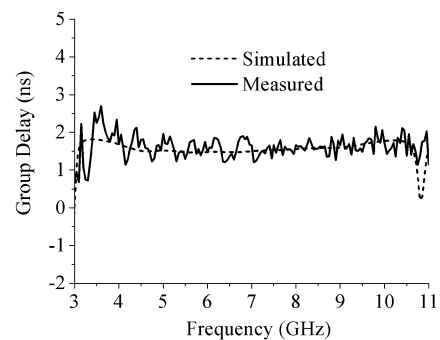


Fig. 13. Simulated and measured group delays of the proposed antenna.

IV. CONCLUSION

A planar printed quasi-Yagi antenna with size reduction is designed and experimentally studied in this communication. The antenna con-

sists of a microstrip line to slotline transition structure, a driver dipole and two parasitic strips. Two extended stubs are symmetrically added to the ground plane. The lower-end VSWR < 2 limitation of the quasi-Yagi antenna with modified ground plane is extended to 3.6 GHz from the original 3.9 GHz. The width of the proposed antenna is reduced by approximately 16.7% compared with the original antenna. A prototype of the antenna is fabricated and tested to demonstrate the effectiveness of the design. The measured results show that the measured bandwidth defined by VSWR < 2 is from 3.6 to 11.6 GHz with a ratio of about 3.22: 1. A good F/B ratio, which is better than 10 dB, is obtained from 3.6 to 10.3 GHz. In addition, the measured group delay of the antenna shows that this planar quasi-Yagi antenna has a good time-domain characteristic, which means that a transmitted signal will not be seriously distorted by using this printed quasi-Yagi antenna.

ACKNOWLEDGMENT

The authors would like to thank D. Bao and C. Wang from the School of Electronic Engineering, University of Electronic Science and Technology of China, for measuring the antenna presented in this communication.

REFERENCES

- [1] S. Lim and H. Ling, "Design of a closely spaced, folded Yagi antenna," *IEEE Antennas Wireless Propag. Lett.*, vol. 5, pp. 302–305, 2006.
- [2] J. Huang and A. C. Demission, "Microstrip Yagi array antenna for mobile satellite vehicle application," *IEEE Trans. Antennas Propag.*, vol. 39, no. 7, pp. 1024–1030, Jul. 1991.
- [3] E. Avila-Navarro, A. Segarra-Martinez, J. Carrasco, and C. Reig, "A low-cost compact uniplanar quasi-Yagi printed antenna," *Microwave Opt. Technol. Lett.*, vol. 50, no. 3, pp. 731–735, Mar. 2008.
- [4] S. H. Sedighy, A. R. Mallahzadeh, M. Soleimani, and J. Rashed-Mohassel, "Optimization of printed Yagi antenna using invasive weed optimization (IWO)," *IEEE Antennas Wireless Propag. Lett.*, vol. 9, pp. 1275–1278, 2010.
- [5] S. X. Ta, B. Kim, H. Choo, and I. Park, "Wideband quasi-Yagi antenna fed by microstrip-to-slotline transition," *Microwave Opt. Technol. Lett.*, vol. 54, no. 1, pp. 150–153, Jan. 2012.
- [6] W. R. Deal, N. Kaneda, J. Sor, Y. Qian, and T. Itoh, "A new quasi-Yagi antenna for planar active antenna arrays," *IEEE Trans. Microw. Theory Techn.*, vol. 48, no. 6, pp. 910–918, Jun. 2000.
- [7] T.-G. Ma, C.-W. Wang, R.-C. Hua, and J.-W. Tsai, "A modified quasi-Yagi antenna with a new compact microstrip-to-coplanar strip transition using artificial transmission lines," *IEEE Trans. Antennas Propag.*, vol. 57, no. 8, pp. 2469–2474, Aug. 2009.
- [8] H. K. Kan, R. B. Waterhouse, A. M. Abbosh, and M. E. Bialkowski, "Simple Broadband Planar CPW-fed quasi-Yagi antenna," *IEEE Antennas Wireless Propag. Lett.*, vol. 6, pp. 18–20, 2007.
- [9] D. S. Woo, Y. G. Kim, K. W. Kim, and Y. K. Cho, "Design of quasi-Yagi antennas using an ultra-wideband balun," *Microwave Opt. Technol. Lett.*, vol. 50, no. 8, pp. 2068–2071, Aug. 2008.
- [10] S. X. Ta, B. Kim, H. Choo, and I. Park, "Slot-line-fed quasi-Yagi antenna," in *Proc. Int. Symp. on Antennas Propagation and EM Theory*, Dec. 2010, pp. 307–310.
- [11] K. Han, Y. Park, H. Choo, and I. Park, "Broadband CPS-fed Yagi-Uda antenna," *Electron. Lett.*, vol. 45, no. 24, Nov. 2009.
- [12] R. A. Alhalabi and G. M. Rebeiz, "Differentially-fed millimeter-wave Yagi-Uda antennas with folded dipole feed," *IEEE Trans. Antennas Propag.*, vol. 58, no. 3, pp. 966–969, Mar. 2010.
- [13] S. X. Ta, S. Kang, and I. Park, "Closely spaced two-element folded-dipole-driven quasi-Yagi array," *J. Electromagn. Engrg. Sci.*, vol. 12, no. 4, pp. 254–259, Dec. 2012.
- [14] P. T. Nguyen, A. Abbosh, and S. Crozier, "Wideband quasi-Yagi antenna with tapered driver," in *Proc. Asia-Pacific Conf. on Antennas and Propagation*, Singapore, Aug. 2012, pp. 138–139.
- [15] K. Jiang, Q. G. Guo, and K. M. Huang, "Design of a wideband quasi-Yagi microstrip antenna with bowtie active elements," in *Proc. Int. Conf. on Microwave and Millimeter Wave Technology (ICMMT)*, 2010, pp. 1122–1124.

- [16] J. Wu, Z. Zhao, Z. Nie, and Q.-H. Liu, "A broadband unidirectional antenna based on closely spaced loading method," *IEEE Trans. Antennas Propag.*, vol. 61, no. 1, pp. 109–116, Jan. 2013.
- [17] P. Fei, Y.-C. Jiao, W. Hu, and F.-S. Zhang, "A miniaturized antipodal Vivaldi antenna with improved radiation characteristics," *IEEE Antennas Wireless Propag. Lett.*, vol. 10, pp. 127–130, 2011.

Quality Factor and Radiation Efficiency of Dual-Mode Self-Resonant Spherical Antennas With Lossy Magnetodielectric Cores

Troels V. Hansen, Oleksiy S. Kim, and Olav Breinbjerg

Abstract—For spherical antennas consisting of a solid magnetodielectric lossy core with an impressed surface current density exciting a superposition of the TE_{mn} and TM_{mn} spherical modes, we analytically determine the radiation quality factor Q and radiation efficiency e . Also, we determine the relative mode excitation, as a function of the core material parameters, which ensures self-resonance. For the specific case of a dual- TE_{m1} , TM_{m1} dipole antenna of half a wavelength circumference, we show quantitatively, how Q/e and e behave, and can be optimized as functions of permeability and magnetic loss tangent. We obtain Q/e values well below the Chu lower bound with fair efficiencies up to 71% – 84%.

Index Terms—Electrically small antennas, energy storage, magnetic losses, quality factor, spherical antennas.

I. INTRODUCTION

Many have endeavoured to determine and approach the fundamental lower-bound upon the radiation quality factor Q of electrically small antennas, e.g., [1]–[6]. Chu [3] studied a spherical volume of radius a circumscribing the antenna, expanded the external fields as spherical TE_{mn} and TM_{mn} modes,¹ assumed zero internal stored energy, and found that the electric or magnetic dipole fields yielded the lowest Q , this Chu lower bound is

$$Q_{Chu} = \frac{1}{(k_0 a)^3} + \frac{1}{k_0 a} \quad (1)$$

where k_0 is the free-space wavenumber. The Chu lower bound on Q applies for single-mode antennas; McLean [6] showed that the minimum Q for a dual- TE_{m1} , TM_{m1} dipole antenna (i.e., assuming zero internal energy) is

$$Q_{min} = \frac{1}{2(k_0 a)^3} + \frac{1}{k_0 a} \quad (2)$$

which can also be obtained from the earlier results of Fante [5], and for $k_0 a \rightarrow 0$, Q_{min} becomes half of Q_{Chu} as already noted by Chu [3]. It

Manuscript received August 21, 2013; accepted September 11, 2013. Date of publication October 25, 2013; date of current version December 31, 2013.

The authors are with the Department of Electrical Engineering, Technical University of Denmark, Kgs. Lyngby DK-2800, Denmark (e-mail: tvh@elektro.dtu.dk; osk@elektro.dtu.dk; ob@elektro.dtu.dk).

Color versions of one or more of the figures in this communication are available online at <http://ieeexplore.ieee.org>.

Digital Object Identifier 10.1109/TAP.2013.2287290

¹with azimuthal index m , and polar index n .